



Quantitative aspects of ToF-SIMS analysis of metals and alloys in a UHV, O₂ and H₂ atmosphere

Jernej Ekar^{a,b,*}, Saša Kos^{c,d}, Janez Kovač^{a,*}

^a Jožef Stefan Institute, Jamova cesta 39, Ljubljana SI-1000, Slovenia

^b Jožef Stefan International Postgraduate School, Jamova cesta 39, Ljubljana SI-1000, Slovenia

^c Geological Survey of Slovenia, Dimičeva ulica 14, Ljubljana SI-1000, Slovenia

^d Faculty of Civil and Geodetic Engineering, University of Ljubljana, Jamova cesta 2, Ljubljana SI-1000, Slovenia

ARTICLE INFO

Keywords:

ToF-SIMS quantification
H₂ and O₂ gas flooding
Matrix effect reduction
Cluster secondary ions

ABSTRACT

Although secondary ion mass spectrometry (SIMS) is a versatile method used in the fields of surface analysis, depth profiling and elemental and molecular mapping, it also lacks quantification capabilities. The main reason for this is the matrix effect, which influences the ionization yield of secondary ions with respect to the substrate from which the analyzed compounds originate. There are several approaches to reduce the matrix effect, and gas flooding is one of the easiest methods to apply. In this work, we have investigated the possibilities of the ToF-SIMS method for the quantification of selected metals and alloys containing these metals in different ratios by reducing the matrix effect in the presence of different atmospheres. The measurements were performed in the ultra-high vacuum (UHV) environment, H₂ and O₂ atmospheres. H₂ flooding shows the most significant improvements compared to the UHV analysis, while O₂ is also promising but has some limitations. Improvements are most evident for the transition metals Ti, Cr, Fe, Co and Ni employed in our study, while the p-block elements such as Al and Si do not change so extensively. The deviations from the true atomic ratios of selected transition metals in different alloys reach a maximum of only 46 % when analyzed in the H₂ atmosphere. In contrast, these values are 66 and 228 % for the O₂ atmosphere and UHV environment, respectively. Our results suggest that gas adsorption and consequent formation of a new matrix on the surface, especially in the case of hydrogen, reduces the differences between the different chemical environments and electronic structures of the surface. In this way, the quantitative aspects of the SIMS method can be improved.

1. Introduction

Secondary ion mass spectrometry (SIMS) is an important analytical technique in the fields of surface and materials sciences. The information about the chemical composition and molecular structure of the sample is obtained by bombarding the surface with primary ions (e.g. Bi⁺, Bi₃⁺, Ar⁺) and analyzing secondary ions, that is, charged sputtered particles, with a mass analyzer such as time-of-flight (ToF), magnetic sector, quadrupole, ion trap or orbitrap. [1–3] SIMS is a versatile analytical method as the sample to be analyzed is only required to be compatible with ultra-high vacuum (UHV) and, in the case of ToF-SIMS, also needs to be as flat as possible. [3,4] In addition, we can measure mass spectra, perform 2D mapping and depth profiling, and even generate 3D representations. [5] Due to these factors, SIMS can be used

in many different fields such as corrosion inhibition [6,7], studies of metals, alloys and their properties [8,9], analysis of thin films and multilayers [10–12], studies of organic compounds and polymers [13, 14], investigation of nanoparticles [15,16], microelectronics and photovoltaics [17,18], catalysis [19], detection of dopants and impurities [20,21], analysis of biological material including cells and tissues [22, 23] and so on. However, one of the major limitations of the SIMS method is the problematic and often impossible quantification of chemical composition, mainly as a result of the matrix effect. [24–26] The intensity of the secondary ion signal (I_m) is a function of the current of the primary ions (I_p), the sputter yield (Y_m), the ionization probability ($\alpha^{+/-}$), the concentration of an analyzed compound or element (θ_m), and the transmission of the analytical system (η), as described in Eq. (1). [2]

$$I_m = I_p Y_m \alpha^{+/-} \theta_m \eta \quad (1)$$

* Corresponding authors.

E-mail addresses: jernej.ekar@ijs.si (J. Ekar), janez.kovac@ijs.si (J. Kovač).

<https://doi.org/10.1016/j.surfin.2024.104408>

Received 13 December 2023; Received in revised form 27 March 2024; Accepted 25 April 2024

Available online 25 April 2024

2468-0230/© 2024 The Authors. Published by Elsevier B.V. This is an open access article under the CC BY license (<http://creativecommons.org/licenses/by/4.0/>).

I_p and η are functions of an instrument and as such are not problematic since they can be determined and controlled, while θ_m is the concentration we are looking for in the case of quantification. Challenging in terms of quantitative analysis are Y_m and $\alpha^{+/-}$. Even the sputter yield of the element and its ionization probability influenced by its ionization energy and electron affinity are not problematic since they do not change with respect to the sample. [2] The most difficult to overcome is the influence of the substrate, i.e. the matrix effect. This is because the chemical composition of the sample has a large influence on the sputter yield and the ionization probability, and this factor changes from one sample to another, preventing and disrupting direct comparison between them. [2,24]

Various approaches have already been developed to improve and solve this issue. One possibility is the application of laser postionization of secondary neutral sputtered particles (laser-SNMS), an effective but also complicated and costly approach. [27–30] Instead of a laser, we can also use an electron beam. [31–33] Since the particles are ionized in the plume above the surface, in the gas phase, the effect of the substrate matrix is no longer present. [27,34] However, the laser must be strong enough to ionize all targeted particles, otherwise quantification is not possible. [27] We can also use the internal standard method by comparing the intensity of the signal of interest with the intensity of the reference signal and calculating the relative sensitivity factor (RSF) using Eq. (2),

$$c_i/c_r = RSF(I_i / I_r) \quad (2)$$

where c represents the atomic or molar concentration, I the intensity of the secondary ion signal, and the subscripts i and r the element of interest and the internal reference, respectively. [25,35–37] However, this method can only be used if we have samples with a very similar matrix that all contain the element used as an internal standard. [35,36] Another approach involves reactive sputtering, mainly with Cs^+ ions. During the sputtering process, Cs^+ ions are implanted into the substrate, chemically altering it and reducing the work function, thereby promoting the formation of negative secondary ions. [24,25,38,39] In this way, we create a matrix that is more similar between different samples, as it is always based on the effect of the implanted Cs. Improved quantification can be achieved by analyzing MCs^+ or MCs_2^- ions, where M is the metal of interest. [35,40,41]

As gaseous molecules and atoms adsorb to the surface, they also form a type of matrix, similarly as with Cs implantation, which modifies the surface even more extensively. Furthermore, a positive effect of an H_2 atmosphere on the differentiation between layers of metals, metal oxides and alloys as well as an optimized identification of interfaces has already been demonstrated by SIMS analyses. [42] Therefore, the intensities of secondary ions sputtered from different metals and alloys were measured and compared in UHV, H_2 and O_2 atmospheres.

A current study aimed to evaluate and optimize a new approach for quantification of SIMS data from metallic alloys in different atmospheres. A relative comparison between pure metal and different alloys containing this metal in different ratios was performed to find the most favorable conditions for reducing/eliminating the matrix effect while applying an H_2 or O_2 atmosphere. Significantly different samples were used so that the matrix effect would play an important role in the quantification. In the present study, we considered different ways of normalizing the acquired SIMS signals and systematically compared the quantification in the H_2 or O_2 atmosphere with the UHV. Our results improved the semi-quantitative aspect of the SIMS method by providing the possibility to compare chemically distinct alloys and metals. However, a relative comparison would still be necessary with reference materials, as a direct correlation of the intensities of the secondary ion signals with the composition of a particular alloy should not be possible. This is due to the large variations in ionization energies, electron affinities and ionization yields of cluster secondary ions between different metals. [24,43,44]

2. Experimental section

2.1. Preparation of the samples

Co, CoCr, NiTi, AlTiV, Fernico, Inconel, Kanthal and stainless steel used in this study were in the form of bulk samples with a homogeneous composition and covered with a thin native oxide layer. They were prepared by melting the metal/alloy. If the surface was not flat enough, it was polished at the ambient conditions. Pure Al, Ti, Cr, Fe, Ni, AlCr alloy and alloys of AlTi and SiTi in two different element ratios were prepared in the form of thin films by physical vapor deposition (PVD). They were deposited in a Sputron triode sputtering system (Balzers Oerlikon). The high-purity targets used as sputtering sources for the preparation of the thin films were initially cleaned for 5 min with plasma inside the PVD sputtering system to remove the native oxide and other impurities on their surface. The CoCrFeMnNi alloy was prepared by the arc-melting process. The highly polished crystalline wafer was used as the pure Si sample.

2.2. EDXS measurements

Polished metal samples of CoCr, NiTi, AlTiV, Fernico, Inconel, Kanthal and stainless steel were analyzed for their chemical composition using the Oxford INCA PentaFET x3 energy dispersive X-ray spectrometer with Si(Li) detector coupled to the JEOL JSM 6490LV scanning electron microscope. The chemical analysis was performed at an accelerating voltage of the electron beam of 20 kV, a working distance of 10 mm and an acquisition time of 45 s over five $100 \times 100 \mu m$ scanning areas. The EDS software (INCA Energy 350) was calibrated for quantification with pre-measured universal standards, according to fitted standard procedure, and referenced to Co for optimization. The EDS data was corrected using the standard ZAF-correction method, which is included in the INCA Energy software.

2.3. XPS measurements

X-ray photoelectron spectroscopy (XPS) was performed with the PHITFA XPS spectrometer from Physical Electronics, USA. The monochromatic X-ray source applied was Al using the K_{α} emission. The analyzed area was 0.4 mm in diameter and the depth of analysis was 3–5 nm. The XPS spectra were measured in the energy range of 0–1200 eV. The elemental composition was determined by measuring the intensity of the 2p spectra of Al, Si, Ti, Cr, Fe, Co and Ni. Depth profiling was performed with the Ar^+ ion beam with an energy of 1 keV (AlCr and both SiTi samples) or 3 keV (both AlTi and CoCrFeMnNi samples) over an area of 3×3 mm. The surface composition was quantified using the XPS peak intensities and considering the relative sensitivity factors specified by the instrument manufacturer [45].

2.4. SIMS measurements

The ToF-SIMS analyses were performed with the TOF.SIMS 5 instrument from IONTOF, Germany. Bi^+ primary ions with an energy of 30 keV were used as the analysis beam. The ion beam was pulsed with a pulse length of 6 ns and the current of the Bi^+ ions was between 1.4 and 1.6 pA. With the settings used, the mass resolution $m/\Delta m$ of the peaks of interest was mostly between 7000 and 9000, while the minimum and maximum were 5000 and 13,000, respectively. The analytical depth was approximately 2 nm and the lateral resolution was around 5 μm . The analyses were performed in a dual-beam depth profiling mode using the 1 keV Cs^+ ion beam for sputtering. The current of the Cs^+ ions was between 60 and 65 nA. The analyses with the Bi^+ primary ions were performed over the $50 \times 50 \mu m$ scanning area (128×128 pixels), which was located in the center of the $400 \times 400 \mu m$ area sputtered with the Cs^+ ions. The secondary ions were analyzed over the m/z range from 0 to 400.

The analyses in the UHV environment were performed at a pressure of approximately 2×10^{-10} mbar, while the pressure during O₂ flooding ranged from 1 to 3×10^{-8} mbar and during H₂ flooding from 5×10^{-7} to 1×10^{-6} mbar. The initial pressure prior to the gas introduction was always in the 10^{-10} mbar range. The differences in the pressures of H₂ and O₂ are pressure fluctuations during a single analysis and not differences between successive measurements of different samples. The gases used during depth profiling were introduced into the analysis chamber near the analyzed region via a capillary. The purity of the gasses used was 99.9990 % and 99.9950 % for O₂ and H₂, respectively.

In order to minimize the effects of the measurement conditions, the samples were analyzed as similarly as possible and in the shortest feasible time span. Since H₂ and O₂ form hydride or oxide cluster ions with the metals, which ionize most effectively in the negative polarity, we only analyzed negative secondary ions. To obtain results that were as comparable as possible, the negative secondary ions were also analyzed during the measurements in the UHV as well. Cs⁺ sputtering was performed simultaneously to further promote the formation of negative secondary ions. The measurement time was determined according to the thickness of the layers in the corresponding samples, so that the measurements were performed in a time interval of 150 s, during which the intensities of the signals of interest remained unchanged. An exception was Fe in the form of the thinnest layer with a measurement time of 90 s. Bulky samples analyzed with the EDXS were additionally sputtered for a longer time of approximately 10 min to check their homogeneity, but no fluctuations in the signal intensities were observed. Prior to the secondary ion intensity measurements, sputtering was also performed to remove the topmost oxide layer or layers above the layer of interest. The results of this process were not included in the intensity ratio calculations. The duration of sputtering prior to analysis was determined in accordance with the sample roughness and the thickness of the oxide layer or the depth at which the layer of interest was located. Depending on the sample, it lasted between 10 and 60 min and was done with the 1 keV Cs⁺ ion beam as well.

3. Results and discussion

3.1. Compositions of the samples and quantification method

Al, Si, Ti, Cr, Fe, Co and Ni were measured as pure metals containing only traces of the other elements. Therefore, we have considered them as 100 % metals in the calculations. We must also emphasize that we are aware that Si is a semimetal, but to avoid complications in sentences, we have only used the terms metal and metals in the text. The exact compositions of alloys were determined using either EDXS or XPS measurements. EDXS was used for the bulk samples, which were CoCr, AlTiV, Fernico, Inconel, Kanthal and stainless steel. Both AlTi, AlCr, both SiTi and CoCrFeMnNi samples were in the form of layers, so they

were analyzed with XPS with high surface sensitivity to avoid the influence of the underlying substrate. Only the NiTi sample was purchased with the certified composition, but it was still measured with EDXS to verify the composition. The measured atomic ratios of alloys are listed in Table 1.

Our samples differ considerably from each other and contain no common element in all of them. The application of the RSF approach and Eq. (2) [35,37] was consequently not possible. Therefore, we used the atomic ratios from Table 1 to prepare our approach for quantification in different measurement conditions. The intensities of the secondary ion signals measured on different alloys were divided by the intensity values of these signals measured on the pure metal. This corresponds to normalization by the theoretical atomic ratio of 1. In this way, comparative intensity ratios between the samples were calculated for each secondary ion. Tables, presented in the Supplementary Information (SI) file and analogous to Table 1, were created from the ToF-SIMS data for all listed alloys and three different atmospheres.

To compare the quantification results, we evaluated the deviations of the intensity ratios of the SIMS secondary ion signals from the true atomic ratios of each element determined by EDXS or XPS. The deviations were calculated using Eq. (3), where Δ indicates the relative errors, the R_m ratios calculated by comparing the measured SIMS intensities of the secondary ions, and the R_t true atomic ratios obtained by EDXS or XPS. The deviations of the secondary ion signals measured on pure metals are always 0 by definition. In addition, all deviation values are noted with the +/- sign, so that one can calculate the exact comparative ratios we measured with the SIMS instrument.

$$\Delta = (R_m - R_t)/R_t \quad (3)$$

Since the measurement of SIMS signals can be sensitive to small changes in the analysis conditions (ion current of the primary ion beam, efficiency of ion detection...) the measured SIMS signal intensities were normalized in three different ways before calculating the R_m ratios. The most straightforward approach was normalization by the total dose of primary Bi⁺ ions. The other option was normalization by the total intensity of all secondary ions hitting the detector. Finally, the signals from spectra measured in the H₂ and O₂ atmospheres were also normalized by the intensity of the H⁻ and O₂⁻ signals, respectively. We chose the O₂⁻ signal instead of the O⁻ signal because the latter was constantly saturated during O₂ flooding and would represent a normalization by the constant.

We also encountered some limitations in the selection of suitable metals. Mn and Mo were not analyzed as they are present in the studied alloys in too low a concentration to perform a reliable analysis, while Mn is present in only one alloy in sufficient quantity, making such an analysis deficient and inadequate. The presence in only one alloy at a low concentration was a limiting factor for V and Nb as well. Another problem with the low concentrations of some metals is the overlap of

Table 1

Atomic ratios of the analyzed elements in different alloys expressed in percent (%). The method used for the analyses of the referenced chemical composition is also indicated.

| | method | Al | Si | Ti | V | Cr | Mn | Fe | Co | Ni | Nb | Mo |
|-----------------|--------|----|----|----|---|------|-----|------|------|------|-----|-----|
| AlTi 30 | XPS | 30 | 0 | 70 | 0 | 0 | 0 | 0 | 0 | 0 | 0 | 0 |
| AlTi 47 | XPS | 47 | 0 | 53 | 0 | 0 | 0 | 0 | 0 | 0 | 0 | 0 |
| AlCr | XPS | 37 | 0 | 1 | 0 | 62 | 0 | 0 | 0 | 0 | 0 | 0 |
| SiTi 31 | XPS | 0 | 31 | 69 | 0 | 0 | 0 | 0 | 0 | 0 | 0 | 0 |
| SiTi 51 | XPS | 0 | 51 | 49 | 0 | 0 | 0 | 0 | 0 | 0 | 0 | 0 |
| CoCr | EDXS | 0 | 1 | 0 | 0 | 31 | 1 | 0 | 63.5 | 0 | 0 | 3.5 |
| NiTi | EDXS | 0 | 0 | 50 | 0 | 0 | 0 | 0 | 0 | 50 | 0 | 0 |
| AlTiV | EDXS | 10 | 0 | 87 | 3 | 0 | 0 | 0 | 0 | 0 | 0 | 0 |
| Fernico | EDXS | 0 | 0 | 0 | 0 | 0 | 0.5 | 54 | 17.5 | 28 | 0 | 0 |
| Inconel | EDXS | 0 | 0 | 0 | 0 | 26 | 0 | 2 | 0 | 64.5 | 2.5 | 5 |
| Kanthal | EDXS | 10 | 0 | 0 | 0 | 22.5 | 0 | 67.5 | 0 | 0 | 0 | 0 |
| stainless steel | EDXS | 0 | 1 | 0 | 0 | 19 | 1.5 | 65 | 0 | 12 | 0 | 1.5 |
| CoCrFeMnNi | XPS | 0 | 0 | 0 | 0 | 19 | 19 | 21.5 | 24 | 16.5 | 0 | 0 |

their low-intensity SIMS signals with other, more intense signals and the consequent significant errors in the readings. The Ti in the AlCr sample was not included in the calculations for this reason. Fe, on the other hand, has sufficiently strong signals for reliable analysis even when present at only 2 % (Inconel), but there are limitations associated with some specific hydride and oxide signals. An example of a signal-abundant mass interval is shown in Fig. 1. Superimposed are the spectra of the Fernico alloy and the metals Fe, Co and Ni it contains, measured in an H₂ atmosphere. The signals of Si in CoCr and stainless steel were also intense enough for analysis, although the proportion of Si in these alloys is only 1 %. However, when the differences in the ratios of an element in different samples are as large as between 1 and 100 %, this leads to problems in selecting the appropriate signals for analysis. Signals that are of ideal intensity in pure Si are extremely weak in CoCr and stainless steel and are affected by noise, while signals that are intense enough in both alloys are saturated or nearly saturated in pure Si. For this reason, we had to analyze the ²⁹Si⁻ ion instead of the Si⁻ ion.

Dosing the analysis chamber with different gasses and at different pressures during the SIMS analyses results in different intensities of the emitted signal of ions. In the first phase of our study, the pressures of the H₂ and O₂ atmospheres were chosen so that the analyses were carried out as much as possible in the “saturated” region. The small pressure changes in this pressure interval are not expected to cause a large difference in the intensity of the cluster secondary ions (hydrides and oxides). An example of how the intensity of the cluster secondary ions changes with increasing H₂ pressure is shown in Fig. 2 for the stainless steel sample. It can be seen that the increasing pressure initially causes an increase in the intensity of the cluster secondary ions, followed by a slight plateau at approximately 1 × 10⁻⁶ mbar, and ends with a decrease in intensity. The pressure at which this plateau occurs is slightly different for the different metals, but the differences are small enough that optimal pressure can be chosen. The results of the same-approach experiment performed in the O₂ atmosphere are shown in SI in Fig. 3, where it can be seen that the complexity of the intensity changes is much greater in this case. Some oxide signals show a very sharp maximum

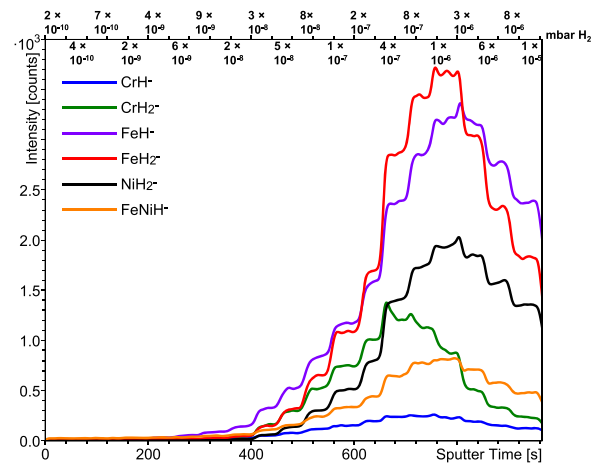


Fig. 2. Changes in the intensity of metal hydride secondary ions emitted from the stainless steel sample during a steady increase of the H₂ pressure inside the analysis chamber to 1 × 10⁻⁵ mbar. For the first 50 s, the pressure was 2 × 10⁻¹⁰ mbar (UHV), then the leak valve was opened slightly every 50 s. The pressures measured between turns of the valve are noted on the upper x-axis, while the lower x-axis shows the time of analysis. The NiH₂ signal was multiplied by a factor of 0.3 to avoid too large differences in the intensities of the different signals.

instead of a plateau, while others have a minimum at this pressure. Furthermore, maxima and plateaus can be observed at significantly different pressures and some oxides even show double maxima/plateaus depending on the O₂ pressure. These limitations compromise the ability to choose an ideal pressure and have a negative impact on the quantification results.

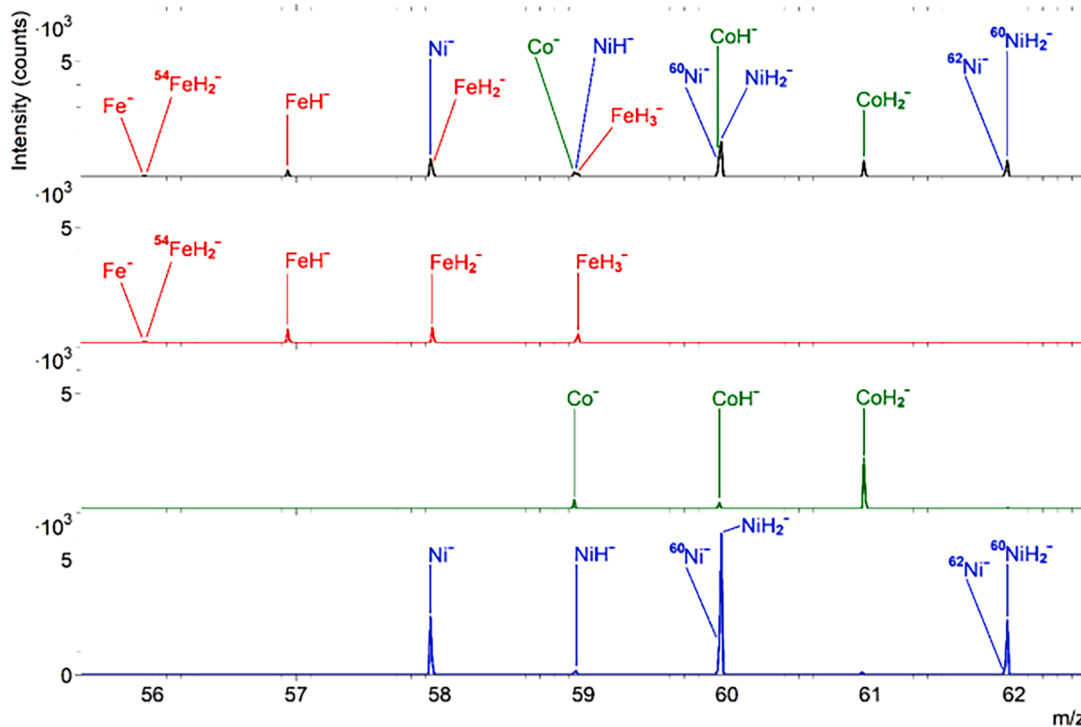


Fig. 1. The SIMS spectra of the negative secondary ions from Fernico alloy (black), Fe (red), Co (green) and Ni (blue) acquired in an H₂ atmosphere. The spectral range between the masses 55.5 and 62.5 is shown, in which the signals of Fe, Co, Ni and their hydrides are present. The intensity of the signals of these secondary ions reflects the concentration of certain elements in the Fernico alloy.

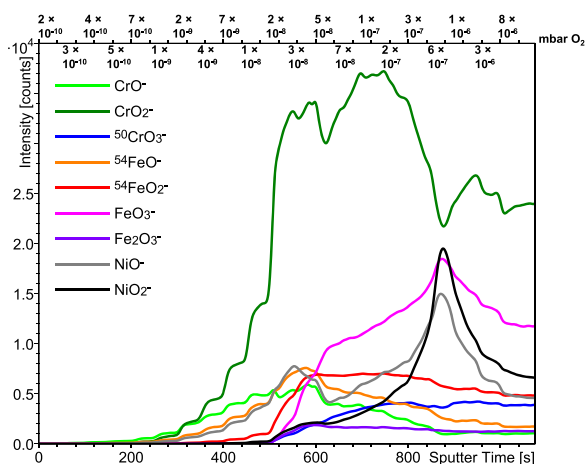


Fig. 3. Changes in the intensity of metal oxide secondary ions emitted from the stainless steel sample during a steady increase of the O₂ pressure inside the analysis chamber to 8×10^{-6} mbar. For the first 50 s, the pressure was 2×10^{-10} mbar (UHV), then the leak valve was opened slightly every 50 s. The pressures measured between turns of the valve are noted on the upper x-axis, while the lower x-axis shows the time of analysis.

3.2. SIMS analyses in UHV environment

The first set of results was obtained in the UHV environment, as this is the conventional way of performing SIMS measurements. In UHV, the secondary ions that were intense enough for reliable analysis were

monoatomic and diatomic metal ions (M^- and M_2^-). Among diatomic secondary ions, Al_2^- , Si_2^- , Ti_2^- and Cr_2^- were suitable and intense enough for analysis, while the signals of Fe, Co and Ni had interferences mainly from mixed metal ions. Mass analyzers with a higher resolving power such as orbitrap, FT-ICR or magnetic sector are mainly able to discriminate between these ions, but ToF analyzers with the reflectron lack this capability in most cases, as the required mass resolution $m/\Delta m$ is at least 25 000. [46] Since these analyses were performed without the presence of a gas, we could only normalize the intensities of the secondary ions of interest by either the total dose of the primary Bi^+ ions or by the total intensity of all secondary ions. Deviation intervals, expressing the deviations of the comparative ratios of the secondary ion signals from the true atomic ratios, are shown in Fig. 4 as intervals between the highest negative and the highest positive deviation when considering all alloys containing a metal of interest. The results are presented in separate graphs for each type of normalization and only one secondary ion represents each element. It was selected according to the criterion of the smallest deviation interval among all secondary ions analyzed. A list of all these secondary ions together with the deviation values measured separately for each alloy is presented in SI in Tables S1 and S2.

The deviation intervals also have their uncertainties, but we can only approximate them because of their complexity. This is the reason why the columns in the diagrams are shown without error bars. The uncertainties in the deviation intervals are related to intrinsic errors of the reference techniques (EDXS and XPS), changes in Bi^+ and Cs^+ primary ion currents and gas pressure during SIMS measurements, mixing of layers in multilayered samples, determination of the signal area and repeatability errors when considering repetitions of measurements of

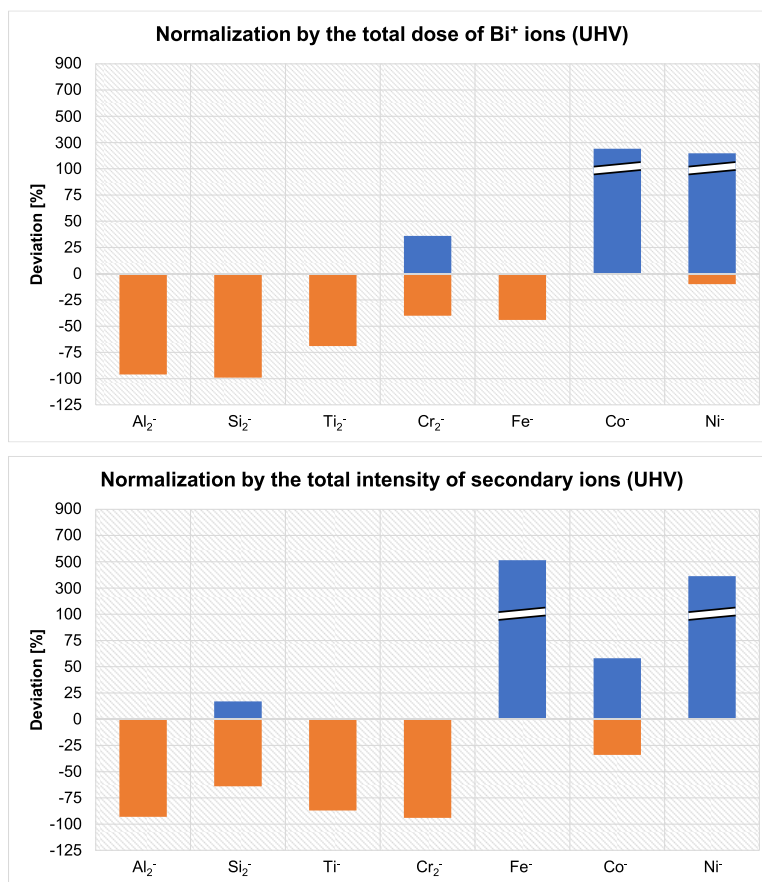


Fig. 4. Deviation intervals between the highest negative and the highest positive deviation from the atomic ratios listed in Table 1 for measurements in the UHV environment. Each element is represented by one secondary ion selected on the basis of the smallest deviation interval among all secondary ions analyzed for that element.

the same sample. We assume that the relative uncertainty of the deviation intervals is between $\pm 30\%$ and $\pm 50\%$ of its value. Thus, if the deviation interval is 30% and the worst case scenario with the relative uncertainty of $\pm 50\%$ is considered, this means that the actual deviation interval is between 15% and 45% .

The intensities of the Al_2^- signal are significantly lower than their true values for all alloys, regardless of the type of normalization, as the deviations exceed -90% . The same applies to the Si_2^- signal, which was normalized by the total dose of Bi^+ ions and even reaches a deviation of -99% . The normalization of the same signal by the total intensity of the secondary ions gives slightly better results with an error interval of 81% . Similar to Al_2^- , Ti signals show too low intensities for all alloys. The deviation intervals reach 69% (Ti_2^-) and 87% (Ti^-) for the

normalization by the total dose of Bi^+ ions and the total intensity of all secondary ions, respectively. The deviations of the ratios of the Cr_2^- signal vary depending on the type of normalization used. For the normalization by the total dose of Bi^+ ions, the deviation interval is 76% , while the normalization by the total intensity of secondary ions shows worse results with a deviation interval of 94% completely in the negative direction. The results for the Fe^- signal are even more dependent on the type of normalization. The deviation interval when normalizing by Bi^+ is only 44% , while the normalization by the secondary ions gives an interval of 512% , with all the comparative ratios being higher than their true values. Contrary, in the first case, all ratios are lower than their true values. The Co^- signal also deviates strongly with an interval of 253% when normalization is performed using the

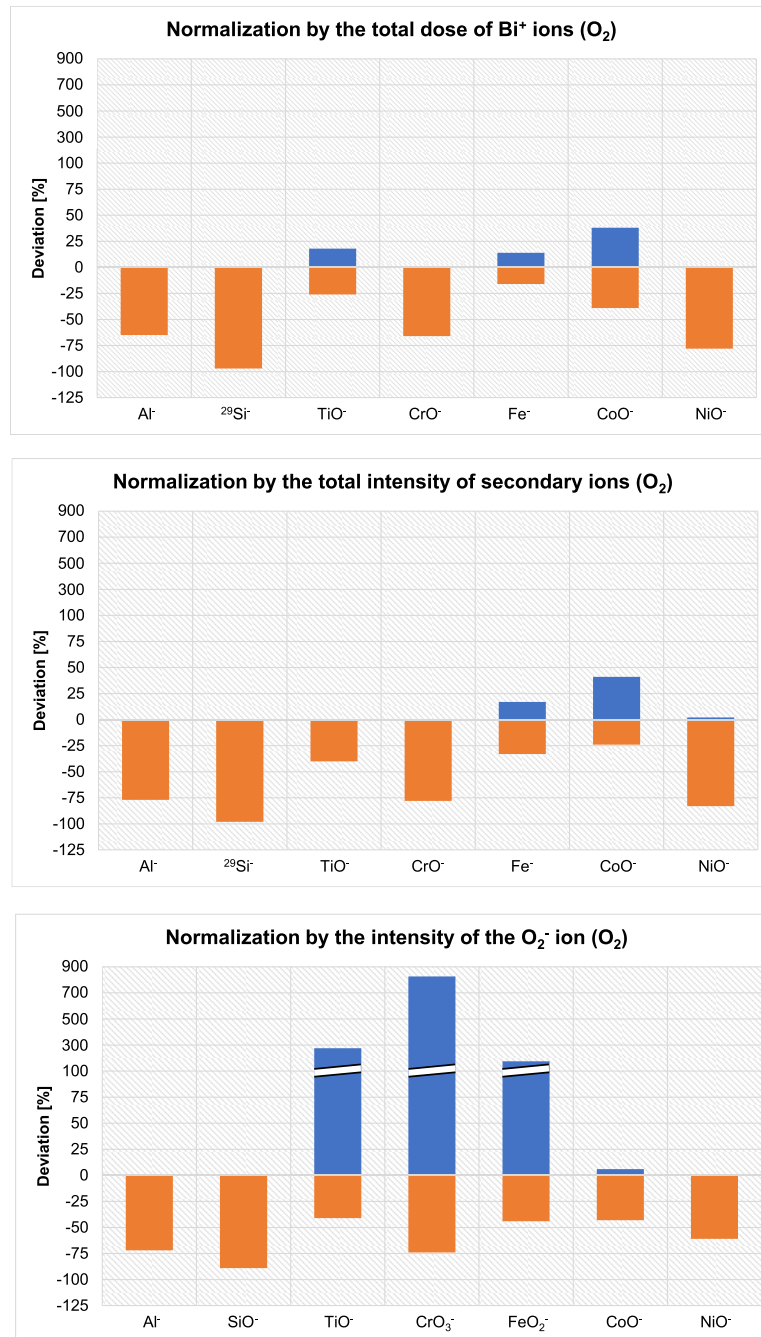


Fig. 5. Deviation intervals between the highest negative and the highest positive deviation from the atomic ratios listed in Table 1 for measurements in the O_2 atmosphere in the pressure range between 1 and 3×10^{-8} mbar. Each element is represented by one secondary ion selected on the basis of the smallest deviation interval among all secondary ions analyzed for that element.

total dose of Bi^+ ions. Normalization by the total intensity of the secondary ions gives slightly better results with a deviation interval of 92 %. The Ni^- signal has deviation intervals of 228 % when normalized by the total dose of Bi^+ and 390 % when normalized by the total intensity of secondary ions.

The results measured in the UHV and normalized by the total dose of Bi^+ ions offer some potential for the quantitative analysis of Fe. Normalization by the total intensity of the secondary ions gives poorer results because no signal has satisfactory deviation intervals. We can conclude that SIMS analysis in the UHV environment is unsuitable for quantification in the vast majority of cases. Such results were to be expected as the substrate, which differs significantly between the different samples, causes a significant matrix effect that prevents successful quantification. Another substantial factor is a limited selection of signals suitable for analysis. For the signals of Fe, Co and Ni there were no alternatives as only M^- signals were an option, whereas for Al, Si, Ti and Cr we were able to choose between M^- and M_2^- ions. This issue is at least partially solved when a reactive atmosphere is introduced, as the cluster ions that are formed provide a wider range of signals that can be used for the calculations.

3.3. SIMS analyses in O_2 atmosphere

Analyses in the O_2 atmosphere are a common practice in the SIMS community to improve the detection of positive secondary ions due to the increased ionization probability in the positive polarity [47]. In our study, we were more interested in a possible quantification of the negative secondary ions, mainly oxides, measured in the O_2 atmosphere during Cs^+ sputtering. Since Cs implantation significantly improves the yield of negative secondary ions [24,25,38,39], we considered only these for analysis. In the following, we compare the quality of three types of normalization of SIMS signals measured in the O_2 atmosphere.

The secondary ions analyzed were monoatomic and diatomic metal ions (M^- and M_2^-), metal oxides, dioxides and trioxides (MO^- , MO_2^- and MO_3^-), and dimetal oxides, dioxides, trioxides and tetraoxides (M_2O^- , M_2O_2^- , M_2O_3^- and M_2O_4^-). The presence of adsorbed oxygen molecules, which significantly alter the initial metallic substrate and influence the matrix effect, together with the wider arrangement of secondary ions available for analysis, led to better results than in the UHV environment. Normalization by the total dose of Bi^+ ions and the total intensity of secondary ions showed promising results for some metals, while normalization by the intensity of the O_2^- signal was not as successful. The results for all three normalizations are shown in Fig. 5. Once more, only the secondary ion with the smallest deviation interval among all secondary ions originating from each element was analyzed. All analyzed signals and their deviation values for each alloy containing this element are listed in SI in Tables S3, S4 and S5.

All comparative ratios of the Al^- signal are lower than their true values, just as in the case of the UHV analysis. However, the deviations are smaller in this case, with the best result observed when normalized by the total dose of Bi^+ ions (−65 %). This is also the smallest measured deviation interval for any type of Al secondary ions that applies to all three types of atmospheres. In the case of Si, both the $^{29}\text{Si}^-$ and SiO^- signals in the alloys exhibit intensities well below their true values regardless of the type of normalization applied. The deviations reach and exceed −90 % in all three cases. The only exception is the SiO^- ion in the CoCr sample with a deviation of 1 % when normalized by the O_2^- signal. The results of the TiO^- signal are much better, at least when normalized by the total dose of Bi^+ ions and the intensity of all secondary ions, with deviation intervals of 44 and 40 %, respectively. The deviation interval in the case of normalization by the O_2^- signal is much larger, 316 %. When normalized by the total Bi^+ dose, a good result is also observed for the Ti_2O^- signal with a deviation interval of 46 %. The deviation intervals of the CrO^- signal are relatively high, reaching 66 and 78 % for the normalization by the total dose of Bi^+ and the total intensity of all secondary ions, respectively. All comparative ratios are

lower than their true values. When normalizing by the intensity of the O_2^- signal, the smallest deviation interval was observed for the CrO_3^- ion, but the interval still reached 900 %. The analysis of Fe gave similar results to Cr. The deviation intervals of the Fe^- ion are 30 and 50 % for the normalization by the total dose of Bi^+ ions and the intensity of all secondary ions, respectively, while the FeO_2^- signal, normalized by the O_2^- reaches a deviation interval of 219 %. On the other hand, the measurements of Co show a reversed situation. The CoO^- ion has the smallest deviation interval when normalized by the O_2^- signal, only 49 %. Normalizations by the total dose of Bi^+ ions and the intensity of all secondary ions resulted in deviation intervals of 77 and 65 %, respectively. The results of the NiO^- signal do not differ significantly depending on the type of normalization. The deviation intervals are 78, 85 and 61 % for the normalization by the total dose of Bi^+ ions, the intensity of all secondary ions and the intensity of the O_2^- ion, respectively.

We can conclude that normalization by the intensity of the O_2^- signal is a favorable approach only for the analysis of Co with an error interval of 49 %, which is a significant improvement compared to the UHV analysis. The general problem could be a diatomic form of the O_2^- ion molecule, but the O^- ion was not an option for normalization due to the constant saturation of this ion during the analysis of all samples in the O_2 atmosphere. Normalization by the total dose of Bi^+ and the total intensity of all secondary ions gives favorable results for Ti and Fe. The deviation intervals for none of these two metals exceed 50 %, which again represents a significant improvement compared to the UHV analysis, where only the Fe^- ion, normalized by the total dose of Bi^+ , has an error interval below 50 %. A substantial improvement compared to the UHV environment is also observed for Ni, but the error intervals remain relatively large. The analysis of Cr in the O_2 atmosphere offers almost no improvement compared to UHV, while the results for Si even deteriorate when O_2 is flooded. Finally, the error intervals for Al decrease compared to the UHV results and the normalization by the total dose of Bi^+ ions gives the smallest error interval among all three atmospheres tested, but remains relatively high with a value of 65 %.

3.4. SIMS analyses in H_2 atmosphere

As a third choice of atmosphere during the SIMS analyses, H_2 flooding was applied as a novel approach. We used just under 1×10^{-6} mbar of H_2 working pressure to maximize the yield of negative metal hydride ions for a few different metals. The secondary ions available for analysis in the H_2 atmosphere were monoatomic and diatomic metal ions (M^- and M_2^-) and their mono-, di- and trihydrides (MH^- , MH_2^- , MH_3^- , M_2H^- and M_2H_2^-). Adsorbed hydrogen further improves the semi-quantitative nature of the SIMS method compared to oxygen, as the deviation intervals of the comparative ratios of all transition metals remain below 50 %. Similar to O_2 , three different types of normalization were applied. Normalization by the total dose of Bi^+ ions gives the best results for Si and Ti, while normalization by the intensity of the H^- ion gives the best results for Al, Fe, Co and Ni. Cr has practically the same deviation interval for both of these normalizations. The results for normalization by the total intensity of all secondary ions are considerably worse. The deviation intervals calculated for all three types of normalization are shown in Fig. 6, while the deviations of the comparative ratios of all analyzed secondary ions for each alloy are listed in SI in Tables S6, S7 and S8.

Al is the only metal for which all deviation intervals are larger than those measured in UHV and O_2 atmosphere. The normalization of the Al^- signal by the total dose of Bi^+ ions results in a deviation interval of 229 %, the total intensity of all secondary ions in a deviation interval of 123 % and the intensity of the H^- ion in a deviation interval of 94 %. All other six investigated metals have the smallest deviation intervals measured during the H_2 flooding compared to the UHV and O_2 atmosphere. However, in the case of Si, it is still relatively large with a value of 72 % when the $^{29}\text{Si}^-$ ion is normalized by the total dose of Bi^+ ions.

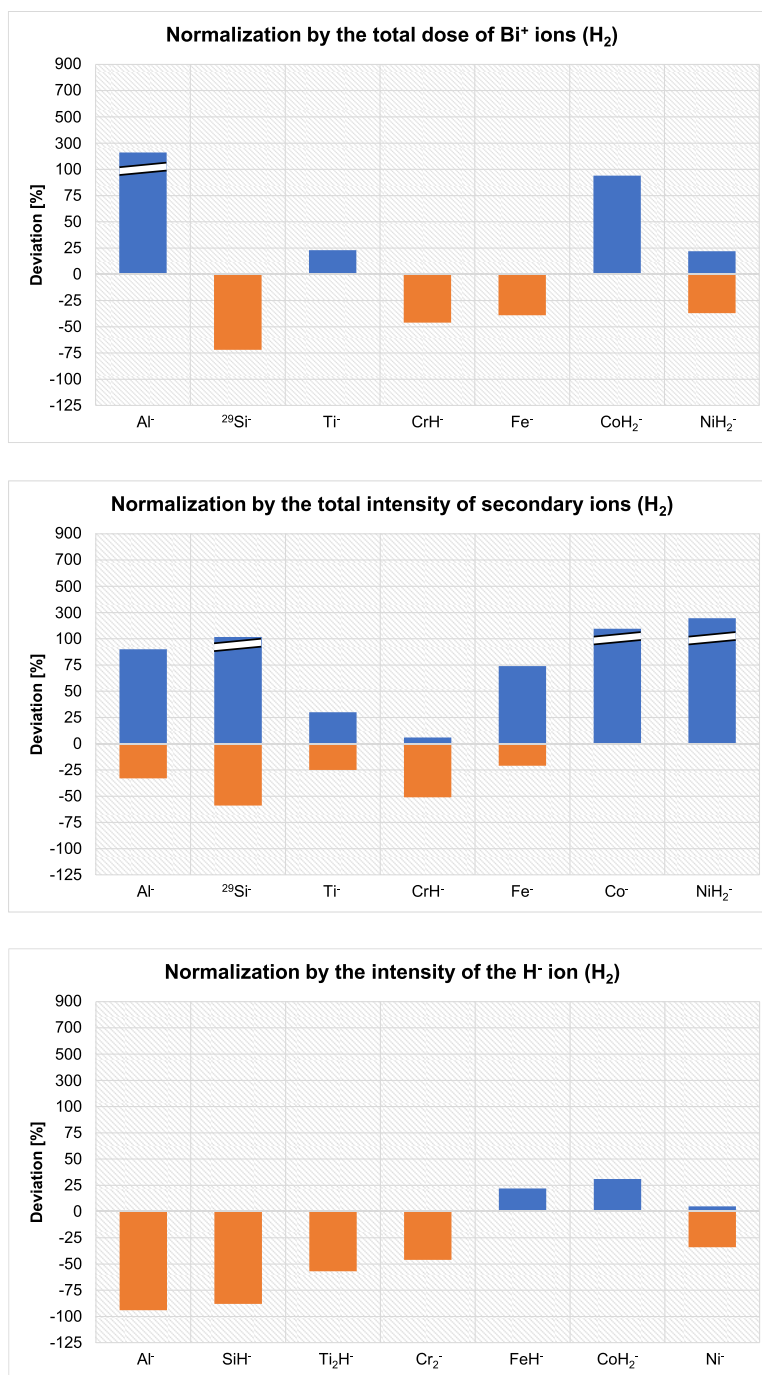


Fig. 6. Deviation intervals between the highest negative and the highest positive deviation from the atomic ratios listed in Table 1 for measurements in the H₂ atmosphere in the pressure range between 5×10^{-7} and 1×10^{-6} mbar. Each element is represented by one secondary ion selected on the basis of the smallest deviation interval among all secondary ions analyzed for that element.

The same type of normalization gives much better results for the Ti⁻ signal with a deviation interval of only 23 %. Normalizations of the Ti⁻ ion by the total intensity of the secondary ions and of the Ti₂H⁻ ion by the intensity of the H⁻ signal give slightly worse, but still good results, 55 and 57 %, respectively. The deviation intervals for Cr are almost the same when normalized by the total dose of Bi⁺ ions and the intensity of the H⁻ ion. In the first case, the CrH⁻ ion has a deviation interval of 46 % and in the second case, the Cr₂⁻ ion reaches an interval of 47 %. The normalization based on the intensity of the H⁻ ion also shows good results for the CrH⁻ ion with a deviation interval of 50 %. The same secondary ion gives a deviation interval of 57 % when normalized by the

total intensity of the secondary ions. The FeH⁻ signal has a deviation interval of only 22 % when normalized by the intensity of the H⁻ ion, while the Fe⁻ signal reaches 40 % when normalized by the intensity of the H⁻ ion, and 95 % when normalized by the total dose of Bi⁺ ions and 177 % when normalized by the total intensity of the secondary ions. The smallest deviation of the CoH₂⁻ signal is observed when normalized by the intensity of the H⁻ ion with an interval of only 31 %. The normalization of that same ion by the total dose of Bi⁺ ions shows a deviation interval of 94 % and the normalization of the Co⁻ ion by the total intensity of the secondary ions shows an interval of 177 %. The normalization by the total intensity of the secondary ions also gives by far the worst result in the analysis of Ni with a deviation interval of 257

%). For the other two Ni options, the deviation intervals are much smaller, 59% when normalizing NiH_2^- ion by the total dose of Bi^+ and 39% when normalizing Ni^- ion by the intensity of the H^- ion.

3.5. Comparison of UHV, O_2 and H_2 atmospheres for the quantification aspect of the SIMS method

We have shown that different secondary ions can be considered for quantification depending on the atmosphere used (oxides or hydrides) and the type of normalization. The secondary ions with the smallest deviation intervals are the same (Al_2^- , Si_2^- , Cr_2^- , Fe^- , Co^- and Ni^-), regardless of the type of normalization, when the analyses were performed in UHV. The only exception is Ti with both Ti^- and Ti_2^- ions. Differences occurred when the O_2 atmosphere was applied. Normalization by the total dose of Bi^+ ions and the total intensity of all secondary ions gives exactly the same secondary ion sets, whereas when normalized by the intensity of the O_2^- ion, changes in the optimal ions for Si, Cr and Fe can be observed. For analyses in the H_2 atmosphere, the differences are even greater, as only the Al^- ion is the same for all three types of normalization. Nevertheless, the normalizations by the total dose of Bi^+ ions and the total intensity of secondary ions remain very similar, with the only difference being Co, but everything else changes when normalizing by the intensity of the H^- ion. Even more surprising is the fact that Cr and Ni hydrides are the optimal options when normalized by total Bi^+ ion dose and total secondary ion intensity, but when normalized by H^- ion intensity, the optimal ions change to Cr_2^- and Ni^- . However, we do not have sufficient knowledge of the mechanism of secondary ion formation to explain this phenomenon, nor do we have data to elaborate why for some elements the smallest deviations are observed for oxides and hydrides, while for others for pure metal secondary ions.

Considering all three types of analytical conditions and all three types of normalizations, we found that the H_2 atmosphere gives the best results for all metals except Al. Normalization by the intensity of the H^- ion provides the smallest deviation intervals for Fe (22%), Co (31%) and Ni (39%). Cr normalized in this way has a deviation interval of 47%, while normalization by the total dose of Bi^+ ions gives an interval of 46%. This type of normalization, combined with H_2 flooding, gives the smallest deviation intervals for Si (72%) and Ti (23%). As the only exception, Al shows the best results when normalized by the total dose of Bi^+ ions after analysis in the O_2 atmosphere, with a deviation interval of 65%. As observed, the transition metals show significantly better results than Al and Si, by approximately 20% or more in absolute units. We can

therefore conclude that O_2 and especially H_2 atmospheres significantly improve the quantification of transition metals in substantially different alloys, while this is not as applicable for the p-block metals and semi-metals, such as Al and Si in our case. Factors that could contribute to this are the reactivities of the analyzed elements, the differences in the electronic structures between d-orbital transition metals and p-orbital Al and Si, and the mass of these elements, with Al and Si being notably lighter.

Finally, we can compare the deviations of all elements in all alloys together for a given atmosphere and type of normalization. Due to the differences between the elements of the d-block and the p-block, we performed such an analysis only for the transition metals. This approach is illustrated in Fig. 7, where the deviation intervals represent the difference between the highest negative and the highest positive deviation from the true value when all five analyzed transition metals (Ti, Cr, Fe, Co and Ni) in all alloys are considered. We regarded only the secondary ions with the smallest deviation intervals, which are shown in Figs. 4, 5 and 6. Optimal results are again observed for the H_2 atmosphere, as the combined deviation interval for normalization by the intensity of the H^- ion is 88%. Normalization by the total dose of Bi^+ ions after analysis in H_2 and O_2 and normalization by the intensity of the secondary ions after analysis in O_2 give deviation intervals of 140, 116 and 124%, respectively. All other approaches have combined deviation intervals of 300% or more and even reach 900%.

These results demonstrate a beneficial effect of the reactive atmospheres on the semi-quantitative aspect of the SIMS method, at least for the transition metals. Adsorbed gas molecules form a new matrix on the surface of the sample containing hydrogen or oxygen atoms. The matrix effect of this layer, i.e. the influence on the ionization of the emitted monoatomic and cluster secondary ions, is approximately the same regardless of the metal or alloy analyzed. In this way, the matrix effect of the original substrate, as observed prior to the exposure to the reactive gasses, is significantly reduced. This phenomenon is similar to reactive Cs^+ sputtering with implantation of Cs^+ ions [35,40,41] and metal-assisted or matrix-enhanced SIMS [48–51], while only Cs^+ enhancement and a specific approach of in situ metal deposition can be applied in depth profiling in the way that gas flooding can [52].

Since the best results were obtained in the H_2 atmosphere after normalization by the intensity of the H^- signal, the same could happen if normalization by the O^- ion was performed in the O_2 atmosphere. However, such an approach would be very challenging due to the very high ionization yield of the O^- ion, resulting in very high intensity and saturation. A lower transmission to the analyzer could be effective, but

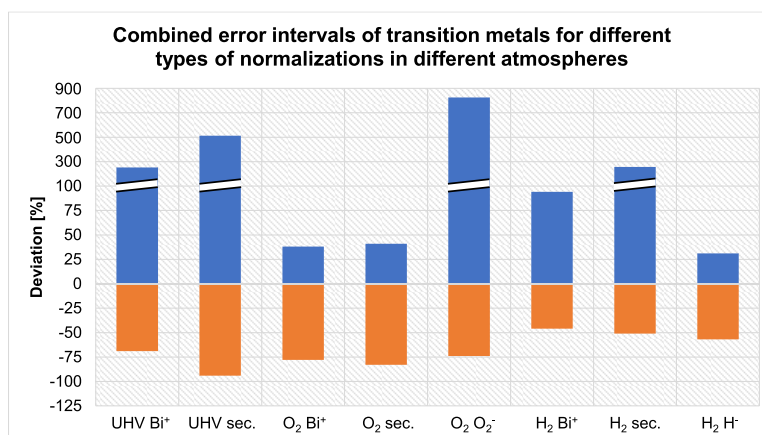


Fig. 7. Combined deviation intervals between the highest negative and the highest positive deviation from the true atomic ratios listed in Table 1 when considering the transition metals (Ti, Cr, Fe, Co and Ni) in all alloys for each type of normalization in each atmosphere. Atmospheres (UHV, O_2 , and H_2) and types of normalization are defined on the x-axis. Bi^+ stands for normalization by the total dose of Bi^+ ions, sec. for normalization by the intensity of all secondary ions, O_2^- for normalization by the intensity of the O_2^- ion, and H^- for normalization by the intensity of the H^- ion.

only if it is applied selectively for the low-mass ions. Otherwise, the intensity of the metal and metal oxide ions would become too low for a reliable analysis. A lower O₂ pressure would be even more problematic, as small changes in O₂ pressure would cause large changes in the intensity of the oxide signals. The intensity of the metal oxide secondary ions would also decrease significantly in this case. Finally, the O₂ atmosphere could be intrinsically problematic as well, since maxima and plateaus of the different oxides differ significantly as a function of O₂ pressure (Fig. 3). Our results showed a dependence of ion signal intensities on gas pressure, suggesting that recombination and cluster secondary ion formation should indeed occur at the surface of the sample or directly above it immediately after the desorption of the particles. [53–57] However, further studies on the mechanism of cluster secondary ion formation are beyond the scope of this work, but are needed to gain a deeper insight and understanding of these processes.

4. Conclusion

Our study shows that reactive atmospheres substantially improve the quantitative capabilities of the SIMS method. This was particularly demonstrated for the transition metals, while the improvements for the p-block elements such as Al and Si are not as significant. The best results were observed for the SIMS analyses in the H₂ atmosphere in combination with the normalizations by the intensity of the secondary H⁻ ion and the total dose of Bi⁺ ions in the primary ion beam. The deviation intervals of the secondary ions of the analyzed transition metals, which had the smallest deviations among all secondary ions originating from the respective metal, were 23 % for Ti, 46 % for Cr, 22 % for Fe, 31 % for Co and 39 % for Ni. These values are significantly better than the results measured in the UHV, where all deviation intervals except for the Fe⁻ ion reached 70 % or more. The Fe⁻ signal normalized by the total dose of Bi⁺ ions gave a deviation interval of 44 %. The results measured during O₂ flooding showed improvements compared to the UHV environment, but not as prominent as for H₂ flooding. In the H₂ atmosphere, we improved the quantitative analysis of transition metals in significantly different alloys consisting of two to five different elements. Furthermore, the atomic ratios of these elements ranged from only a few percent to almost 100 %. This is in contrast to previous SIMS studies quantifying very similar alloys and compounds, composed of the same elements with only minor differences in their relative ratios. For the application of our quantitative approach, a current of Bi⁺ and Cs⁺ ion beams as stable as possible and precise control of the gas pressure in the SIMS analysis chamber are crucial. To improve the proposed quantitative approach, further studies on the mechanisms of hydride and oxide cluster secondary ion formation are needed and planned.

CRediT authorship contribution statement

Jernej Ekar: Writing – review & editing, Writing – original draft, Visualization, Resources, Project administration, Methodology, Investigation, Formal analysis, Conceptualization. **Saša Kos:** Investigation, Formal analysis, Writing – original draft. **Janez Kovač:** Funding acquisition, Project administration, Resources, Supervision, Writing – review & editing.

Declaration of competing interest

The authors declare that they have no known competing financial interests or personal relationships that could have appeared to influence the work reported in this paper.

Data availability

Data will be made available on request.

Acknowledgment

The authors thank prof. Dr. Peter Panjan for preparing the multi-layered samples containing Al, Si, Ti, Cr, Fe, Ni, both AlTi, AlCr, and both SiTi films. We would also like to thank the researcher Barbara Ljubec Božiček for providing the CoCrFeMnNi sample.

Funding

This work was supported by the Slovenian Research and Innovation Agency (ARIS) through the Programs P2-0082 and P1-0025 and the Project PR-09757.

Supplementary materials

Supplementary material associated with this article can be found, in the online version, at doi:10.1016/j.surfim.2024.104408.

References

- [1] P. van der Heide, Sputtering and ion formation. *Secondary Ion Mass Spectrometry An Introduction to Principles and Practices*, John Wiley & Sons, Hoboken, New Jersey, 2014, pp. 44–143.
- [2] J.C. Vickerman, Prologue: ToF-SIMS—an evolving mass spectrometry of materials, in: D. Vickerman (Ed.), *ToF-SIMS Materials Analyses by Mass Spectrometry*, Ed.2nd Ed, IM Publications LLP and SurfaceSpectra Limited, Chichester, Manchester, 2013, pp. 1–37.
- [3] P. van der Heide, Instrumentation used in SIMS. *Secondary Ion Mass Spectrometry An Introduction to Principles and Practices*, John Wiley & Sons, Hoboken, New Jersey, 2014, pp. 147–194.
- [4] B.W. Schueler, Time-of-flight mass analysers, J. C. & Briggs (Ed.), in: D. Vickerman (Ed.), *ToF-SIMS Materials Analyses by Mass Spectrometry*, 2nd Ed, IM Publications LLP and SurfaceSpectra Limited, Chichester, Manchester, 2013, pp. 247–270.
- [5] P. van der Heide, The art of measurement. *Secondary Ion Mass Spectrometry An Introduction to Principles and Practices*, John Wiley & Sons, Hoboken, New Jersey, 2014, pp. 195–208.
- [6] Y. Abe, M. Komatsu, H. Okuhira, Estimation of ToF-SIMS information depth in micro-corrosion analysis, *Appl. Surf. Sci.* (2003) 859–862, [https://doi.org/10.1016/S0169-4332\(02\)00824-3](https://doi.org/10.1016/S0169-4332(02)00824-3), 203–204.
- [7] D.K. Kozlica, J. Ekar, J. Kovač, I. Milošev, Roles of Chloride Ions in the Formation of Corrosion Protective Films on Copper, *J. Electrochem. Soc.* 168 (2021) 031504, <https://doi.org/10.1149/1945-7111/abe34a>.
- [8] P. Jovičević-Klug, N. Lipovšek, M. Jovičević-Klug, M. Mrak, J. Ekar, B. Ambrožič, G. Dražič, J. Kovač, B. Podgornik, Assessment of deep cryogenic heat-treatment impact on the microstructure and surface chemistry of austenitic stainless steel, *Surfaces and Interfaces*. 35 (2022) 102456. <https://doi.org/10.1016/J.SURFIN.2022.102456>.
- [9] X. Xu, C. Jiao, K. Li, M. Hao, K.L. Moore, T.L. Burnett, X. Zhou, Application of high-spatial-resolution secondary ion mass spectrometry for nanoscale chemical mapping of lithium in an Al-Li alloy, *Mater. Charact.* 181 (2021) 111442, <https://doi.org/10.1016/J.MATCHAR.2021.111442>.
- [10] J. Kovač, J. Ekar, M. Čekada, L. Zajčková, D. Nečas, L. Blahová, J. Yong Wang, M. Mozetič, Depth profiling of thin plasma-polymerized amine films using GDOES in an Ar-O₂ plasma, *Appl. Surf. Sci.* 581 (2022) 152292, <https://doi.org/10.1016/J.APSUSC.2021.152292>.
- [11] M. Holzweber, A.G. Shard, H. Jungnickel, A. Luch, W.E.S. Unger, Dual beam organic depth profiling using large argon cluster ion beams, *Surf. Interface Anal.* 46 (2014) 936–939, <https://doi.org/10.1002/SIA.5429>.
- [12] E.I. Vasilkova, A.N. Klochkov, A.N. Vinichenko, N.I. Kargin, I.S. Vasil'evskii, Comparison of the thermal interdiffusion phenomena in InGaAs/GaAs and InGaAs/AlGaAs strained heterostructures, *Surfaces and Interfaces*. 29 (2022) 101766. <https://doi.org/10.1016/J.SURFIN.2022.101766>.
- [13] J. Bailey, R. Havelund, A.G. Shard, I.S. Gilmore, M.R. Alexander, J.S. Sharp, D. J. Scurr, 3D ToF-SIMS imaging of polymer multilayer films using argon cluster sputter depth profiling, *ACS Appl. Mater. Interfaces*. 7 (2015) 2654–2659, https://doi.org/10.1021/AM507663V/SUPPL_FILE/AM507663V_SI_001.PDF.
- [14] A.G. Shard, R. Havelund, M.P. Seah, S.J. Spencer, I.S. Gilmore, N. Winograd, D. Mao, T. Miyayama, E. Niehuis, D. Rading, R. Moellers, Argon cluster ion beams for organic depth profiling: results from a VAMAS interlaboratory study, *Anal. Chem.* 84 (2012) 7865–7873, https://doi.org/10.1021/AC301567T/ASSET/IMAGES/LARGE/AC-2012-01567T_0006.JPEG.
- [15] R.M. Patil, P.P. Deshpande, M. Aalhat, S. Gananadhamu, P.K. Singh, An update on sophisticated and advanced analytical tools for surface characterization of nanoparticles, *Surf. Interfaces* 33 (2022) 102165, <https://doi.org/10.1016/J.SURFIN.2022.102165>.
- [16] A. Gulín, A. Shakhov, A. Vasin, A. Astafiev, O. Antonova, S. Kochev, Y. Kabachii, A. Golub, V. Nadtochenko, ToF-SIMS depth profiling of nanoparticles: chemical structure of core-shell quantum dots, *Appl. Surf. Sci.* 481 (2019) 144–150, <https://doi.org/10.1016/J.APSUSC.2019.03.097>.

- [17] G. Guryanov, T.P. St. Clair, R. Bhat, C. Caneau, S. Nikishin, B. Borisov, A. Budrevich, SIMS quantitative depth profiling of matrix elements in semiconductor layers, *Appl. Surf. Sci.* 252 (2006) 7208–7210, <https://doi.org/10.1016/J.APSUSC.2006.02.254>.
- [18] K. Brecl, M. Jošt, M. Bokalič, J. Ekar, J. Kovač, M. Topič, Are perovskite solar cell potential-induced degradation proof? *Sol. RRL.* 6 (2022) 2100815 <https://doi.org/10.1002/SOLR.202100815>.
- [19] A. Omerzu, R. Peter, D. Jardas, I. Turel, K. Salamon, M. Podlogar, D. Vengust, I. Jelovica Badovinac, I. Kavre Piltaver, M. Petravc, Large enhancement of photocatalytic activity in ZnO thin films grown by plasma-enhanced atomic layer deposition, *Surf. Interfaces* 23 (2021) 100984, <https://doi.org/10.1016/J.SURFIN.2021.100984>.
- [20] F. Hölzel, D. Rolón, J. Bauer, J. Kober, S. Kühne, F. Pietag, D. Oberschmidt, T. Arnold, Reactive ion beam smoothing of rapidly solidified aluminum (RSA) 501 surfaces for potential visible and ultraviolet light applications, *Surf. Interfaces* 38 (2023) 102784, <https://doi.org/10.1016/J.SURFIN.2023.102784>.
- [21] M. Sumiya, A. Tsukazaki, S. Fuke, A. Ohtomo, H. Koinuma, M. Kawasaki, SIMS analysis of ZnO films co-doped with N and Ga by temperature gradient pulsed laser deposition, *Appl. Surf. Sci.* 223 (2004) 206–209, [https://doi.org/10.1016/S0169-4332\(03\)00923-1](https://doi.org/10.1016/S0169-4332(03)00923-1).
- [22] P. Agüi-Gonzalez, S. Jähne, N.T.N. Phan, SIMS imaging in neurobiology and cell biology, *J. Anal. At. Spectrom.* 34 (2019) 1355–1368, <https://doi.org/10.1039/C9JA00118B>.
- [23] J. Brison, N. Mine, N. Wehbe, X. Gillon, T. Tabarrant, R. Sporcken, L. Houssiau, Molecular depth profiling of model biological films using low energy monoatomic ions, *Int. J. Mass Spectrom.* 321–322 (2012) 1–7, <https://doi.org/10.1016/J.IJMS.2012.04.001>.
- [24] P. van der Heide, Secondary ion yields. *Secondary Ion Mass Spectrometry An Introduction to Principles and Practices*, John Wiley & Sons, Hoboken, New Jersey, 2014, pp. 93–121.
- [25] M. Grasserbauer, Quantitative secondary ion mass spectrometry, *J. Res. Natl. Bur. Stand.* 93 (1988) 510, <https://doi.org/10.6028/JRES.093.140>.
- [26] A. Priebe, T. Xie, G. Bürki, L. Pethö, J. Michler, The matrix effect in TOF-SIMS analysis of two-element inorganic thin films, *J. Anal. At. Spectrom.* 35 (2020) 1156–1166, <https://doi.org/10.1039/c9ja00428a>.
- [27] A. Wucher, *Laser post-ionisation—fundamentals*, J. C. & Briggs (Ed.), in: D. Vickerman (Ed.), *ToF-SIMS Materials Analyses by Mass Spectrometry*, 2nd Ed, IM Publications LLP and SurfaceSpectra Limited, Chichester, Manchester, 2013, pp. 217–246.
- [28] L. Breuer, P. Ernst, M. Herder, F. Meinerzhagen, M. Bender, D. Severin, A. Wucher, Mass spectrometric investigation of material sputtered under swift heavy ion bombardment, *Nucl. Instrum. Methods Phys. Res. Sect. B Beam Interact. Mater. Atoms.* 435 (2018) 101–110, <https://doi.org/10.1016/j.nimb.2017.10.019>.
- [29] L. Breuer, N.J. Popczun, A. Wucher, N. Winograd, Reducing the Matrix Effect in Molecular Secondary Ion Mass Spectrometry by Laser Post-Ionization, *J. Phys. Chem. C.* 121 (2017) 19705–19715, <https://doi.org/10.1021/acs.jpcc.7b02596>.
- [30] N.P. Lockyer, *Laser post-ionisation for elemental and molecular surface analysis*, J. C. & Briggs (Ed.), in: D. Vickerman (Ed.), *ToF-SIMS Materials Analyses by Mass Spectrometry*, 2nd Ed, IM Publications LLP and SurfaceSpectra Limited, Chichester, Manchester, 2013, pp. 361–396.
- [31] R. Wilson, J.A. Van Den Berg, J.C. Vickerman, Quantitative surface analysis using electron beam SNMS: calibrations and applications, *Surf. Interface Anal.* 14 (1989) 393–400, <https://doi.org/10.1002/sia.740140617>.
- [32] M. Kopnarski, H. Jenett, *Electron-impact (EI) secondary neutral mass spectrometry (SNMS). Surfaces Thin Film Analyses*, Wiley-VCH Verlag GmbH & Co. KGaA, Weinheim, Germany, 2011, pp. 161–177.
- [33] H. Oechsner, *Electron gas SNMS. Secondary Ion Mass Spectrometry, SIMS V*, Springer, Berlin, 1986, pp. 70–74.
- [34] L. Breuer, H. Tian, A. Wucher, N. Winograd, Molecular SIMS ionization probability studied with laser postionization: influence of the projectile cluster, *J. Phys. Chem. C.* 123 (2019) 565–574, <https://doi.org/10.1021/acs.jpcc.8b10245>.
- [35] V. Karki, M. Singh, Quantitative depth distribution analysis of elements in high alloy steel using MCs⁺-SIMS approach, *Int. J. Mass Spectrom.* 430 (2018) 22–30, <https://doi.org/10.1016/J.IJMS.2018.04.001>.
- [36] P. van der Heide, Data processing. *Secondary Ion Mass Spectrometry An Introduction to Principles and Practices*, John Wiley & Sons, Hoboken, New Jersey, 2014, pp. 248–268.
- [37] H. Satoh, M. Owari, Y. Nihei, Relative sensitivity factors for submicron secondary ion mass spectrometry with gallium primary ion beam, *Jpn. J. Appl. Phys.* 32 (1993) 3616, <https://doi.org/10.1143/JJAP.32.3616/XML>.
- [38] Y. Kudriatsev, A. Villegas, S. Gallardo, G. Ramirez, R. Asomoza, V. Mishurny, Cesium ion sputtering with oxygen flooding: experimental SIMS study of work function change, *Appl. Surf. Sci.* 254 (2008) 4961–4964, <https://doi.org/10.1016/j.apsusc.2008.01.145>.
- [39] Z. Cong, X. Fu, S. Liu, W. Wang, H. Liu, G. Lei, B. Zhao, H. Wu, C. Gao, Enhancing the organic solar cells performances by elevating cesium carboxylate content of graphene oxide based cathode interface layer, *Surfaces and Interfaces.* 31 (2022) 102068. <https://doi.org/10.1016/J.SURFIN.2022.102068>.
- [40] C. Hongo, M. Tomita, M. Suzuki, Quantitative secondary ion mass spectrometry analysis of impurities in GaN and Al_xGa_{1-x}N films using molecular ions MCs⁺ and MCs₂⁺, *Appl. Surf. Sci.* (1999) 306–309, [https://doi.org/10.1016/S0169-4332\(98\)00815-0](https://doi.org/10.1016/S0169-4332(98)00815-0), 144–145.
- [41] Y.J. Jang, S.H. Kim, K.J. Kim, D. Kim, Y. Lee, Comparison of quantitative analyses using SIMS, atom probe tomography, and femtosecond laser ablation inductively coupled plasma mass spectrometry with Si_{1-x}Ge_x and Fe_{1-x}Ni_x binary alloys, *J. Vac. Sci. Technol. B.* 38 (2020) 034009, <https://doi.org/10.1116/6.0000101/591706>.
- [42] J. Ekar, P. Panjan, S. Drev, J. Kovač, ToF-SIMS Depth Profiling of Metal, Metal Oxide, and Alloy Multilayers in Atmospheres of H₂, C₂H₂, CO, and O₂, *J. Am. Soc. Mass Spectrom.* 33 (2022) 31–44, https://doi.org/10.1021/JASMS.1C00218/ASSET/IMAGES/LARGE/JS1C00218_0008.JPEG.
- [43] P. van der Heide, *Electronic Structure of Atoms and Ions. Secondary Ion Mass Spectrometry An Introduction to Principles and Practices*, John Wiley & Sons, Hoboken, New Jersey, 2014, pp. 27–42.
- [44] A. Priebe, I. Utke, L. Pethö, J. Michler, Application of a gas-injection system during the FIB-TOF-SIMS analysis - influence of water vapor and fluorine gas on secondary ion signals and sputtering rates, *Anal. Chem.* 91 (2019) 11712–11722, <https://doi.org/10.1021/acs.analchem.9b02287>.
- [45] J.F. Moulder, W.F. Stickle, P.E. Sobol, K.D. Bomben, *Handbook of X-Ray Photoelectron Spectroscopy*, Physical Electronics Inc., Eden Prairie, Minnesota, 1995.
- [46] P. van der Heide, *Secondary ion columns. Secondary Ion Mass Spectrometry An Introduction to Principles and Practices*, John Wiley & Sons, Hoboken, New Jersey, 2014, pp. 167–191.
- [47] D. Sykes, A. Chew, M. Crapper, R. Valizadeh, The effect of oxygen flooding on the secondary ion yield of Cs in the Cameca IMS 3f, *Vacuum* 43 (1992) 159–162, [https://doi.org/10.1016/0042-207X\(92\)90204-A](https://doi.org/10.1016/0042-207X(92)90204-A).
- [48] J.D. Debord, A. Prabhakaran, M.J. Eller, S.V. Verkhoturov, A. Delcorte, E. A. Schweikert, Metal-assisted SIMS with hypervelocity gold cluster projectiles, *Int. J. Mass Spectrom.* (2013) 28–36, <https://doi.org/10.1016/j.ijms.2013.03.012>, 343–344.
- [49] S.J.B. Dunham, T.J. Comi, K. Ko, B. Li, N.F. Baig, N. Morales-Soto, J.D. Shrouf, P. W. Bohn, J.V. Sweedler, Metal-assisted polyatomic SIMS and laser desorption/ionization for enhanced small molecule imaging of bacterial biofilms, *Biointerphases* 11 (2016) 02A325, <https://doi.org/10.1116/1.4942884>.
- [50] J.J.D. Fitzgerald, P. Kunnath, A.V. Walker, Matrix-enhanced secondary ion mass spectrometry (ME SIMS) using room temperature ionic liquid matrices, *Anal. Chem.* 82 (2010) 4413–4419, <https://doi.org/10.1021/ac100133c>.
- [51] L. Cai, L. Sheng, M. Xia, Z. Li, S. Zhang, X. Zhang, H. Chen, Graphene oxide as a novel evenly continuous phase matrix for TOF-SIMS, *J. Am. Soc. Mass Spectrom.* 28 (2017) 399–408, <https://doi.org/10.1007/s13361-016-1557-z>.
- [52] A. Yamazaki, T. Tobe, S. Akiba, M. Owari, Metal-Assisted SIMS for three-dimensional analysis using shave-off section processing, *Surf. Interface Anal.* 46 (2014) 1215–1218, <https://doi.org/10.1002/sia.5589>.
- [53] H.M. Urbassek, Status of cascade theory, J. C. & Briggs (Ed.), in: D. Vickerman (Ed.), *ToF-SIMS Materials Analyses by Mass Spectrometry*, 2nd Ed, IM Publications LLP and SurfaceSpectra Limited, Chichester, Manchester, 2013, pp. 67–86.
- [54] F. Honda, G.M. Lancaster, Y. Fukuda, J.W. Rabalais, SIMS study of the mechanism of cluster formation during ion bombardment of alkali halides, *J. Chem. Phys.* 69 (1978) 4931–4937, <https://doi.org/10.1063/1.436480>.
- [55] G.M. Lancaster, F. Honda, Y. Fukuda, J.W. Rabalais, Secondary ion mass spectrometry of molecular solids. cluster formation during ion bombardment of frozen water, benzene, and cyclohexane, *J. Am. Chem. Soc.* 101 (1979) 1951–1958, https://doi.org/10.1021/JA00502A004/ASSET/JA00502A004.FP.PNG_V03.
- [56] J. Vlekken, M. D’Olieslaeger, G. Knuyt, W. Vandervorst, L. De Schepper, Investigation of the formation process of MCs⁺-molecular ions during sputtering, *J. Am. Soc. Mass Spectrom.* 11 (2000) 650–658, [https://doi.org/10.1016/S1044-0305\(00\)00130-6](https://doi.org/10.1016/S1044-0305(00)00130-6).
- [57] B. Saha, P. Chakraborty, Secondary ion mass spectrometry of MCs_n⁺ molecular ion complexes, *Nucl. Instrum. Methods Phys. Res. Sect. B Beam Interact. Mater. Atoms.* 258 (2007) 218–225, <https://doi.org/10.1016/J.NIMB.2006.12.172>.